

5-1-2011

Stretchable microelectrode array using room-temperature liquid alloy interconnects

P. Wei

Birck Nanotechnology Center, Purdue University, pwei@purdue.edu

R. Taylor

Stanford University

Z. Ding

Birck Nanotechnology Center, Purdue University

C. Chung

Stanford University

O. J. Abilez

Stanford University

See next page for additional authors

Follow this and additional works at: <http://docs.lib.purdue.edu/nanopub>

 Part of the [Nanoscience and Nanotechnology Commons](#)

Wei, P.; Taylor, R.; Ding, Z.; Chung, C.; Abilez, O. J.; Higgs, G.; Pruitt, B. L.; and Ziaie, Babak, "Stretchable microelectrode array using room-temperature liquid alloy interconnects" (2011). *Birck and NCN Publications*. Paper 1020.
<http://docs.lib.purdue.edu/nanopub/1020>

This document has been made available through Purdue e-Pubs, a service of the Purdue University Libraries. Please contact epubs@purdue.edu for additional information.

Authors

P. Wei, R. Taylor, Z. Ding, C. Chung, O. J. Abilez, G. Higgs, B. L. Pruitt, and Babak Ziaie

Stretchable microelectrode array using room-temperature liquid alloy interconnects

This article has been downloaded from IOPscience. Please scroll down to see the full text article.

2011 J. Micromech. Microeng. 21 054015

(<http://iopscience.iop.org/0960-1317/21/5/054015>)

View [the table of contents for this issue](#), or go to the [journal homepage](#) for more

Download details:

IP Address: 128.46.221.64

The article was downloaded on 26/07/2013 at 19:15

Please note that [terms and conditions apply](#).

Stretchable microelectrode array using room-temperature liquid alloy interconnects

P Wei^{1,2}, R Taylor³, Z Ding^{2,4}, C Chung^{3,5}, O J Abilez⁶, G Higgs³,
B L Pruitt³ and B Ziaie^{1,2}

¹ School of Electrical and Computer Engineering, Purdue University, West Lafayette, IN, USA

² Birck Nanotechnology Center, Purdue University, West Lafayette, IN, USA

³ Department of Mechanical Engineering, Stanford University, Stanford, CA, USA

⁴ Department of Physics, Purdue University, West Lafayette, IN, USA

⁵ Department of Materials Science and Engineering, Stanford University, Stanford, CA, USA

⁶ Department of Bioengineering, Stanford University, Stanford, CA, USA

E-mail: pwei@purdue.edu

Received 17 November 2010, in final form 27 January 2011

Published 28 April 2011

Online at stacks.iop.org/JMM/21/054015

Abstract

In this paper, we present a stretchable microelectrode array for studying cell behavior under mechanical strain. The electrode array consists of gold-plated nail-head pins (250 μm tip diameter) or tungsten micro-wires (25.4 μm in diameter) inserted into a polydimethylsiloxane (PDMS) platform (25.4 \times 25.4 mm^2). Stretchable interconnects to the outside were provided by fusible indium-alloy-filled microchannels. The alloy is liquid at room temperature, thus providing the necessary stretchability and electrical conductivity. The electrode platform can withstand strains of up to 40% and repeated (100 times) strains of up to 35% did not cause any failure in the electrodes or the PDMS substrate. We confirmed biocompatibility of short-term culture, and using the gold pin device, we demonstrated electric field pacing of adult murine heart cells. Further, using the tungsten microelectrode device, we successfully measured depolarizations of differentiated murine heart cells from embryoid body clusters.

(Some figures in this article are in colour only in the electronic version)

1. Introduction

Stretchable electrodes as cell culture platforms have recently garnered particular attention for their utility in studying cellular behavior/response when subjected to mechanical strain [1, 2]. Such response is central to several important pathologies such as traumatic brain injury (TBI), cardiomyopathy, and vascular disorders. The ability to record and stimulate nerve and muscle cell populations while subjecting them to mechanical strain (electromechanical stimulation) can provide insights into mechanisms of the aforementioned diseases. In addition, stretchable electrodes can be used to study stem cell differentiation since it is widely believed that mechanical cues are important in this process [3, 4]. Stretchable microelectrode arrays can also be used *in vivo* in implantable microdevices such as retinal prosthesis and conformal cortical electrodes [1].

Most reported stretchable electrodes are based on the micro-patterning of a thin gold layer sandwiched between two silicone (PDMS) substrates [5–7]. While using these methods, small sensing/stimulating sites can be defined to achieve high spatial resolution, but electrode impedance values that increase with strain can become exceedingly large (>850 $\text{k}\Omega$) for most sensing and stimulation applications [2]. Other techniques such as pre-stretching PDMS substrates to create buckled gold films [8, 9] and patterning metal interconnections on wavy compliant substrates have also been reported, but these electrodes are not very robust and the fabrication yields are typically low.

In this paper, we present a stretchable cell culture platform with integrated microelectrodes that alleviates the abovementioned problems. This is done by using a room-temperature liquid alloy as interconnects and miniature gold nail-head pins or tungsten micro-wires as electrodes. With

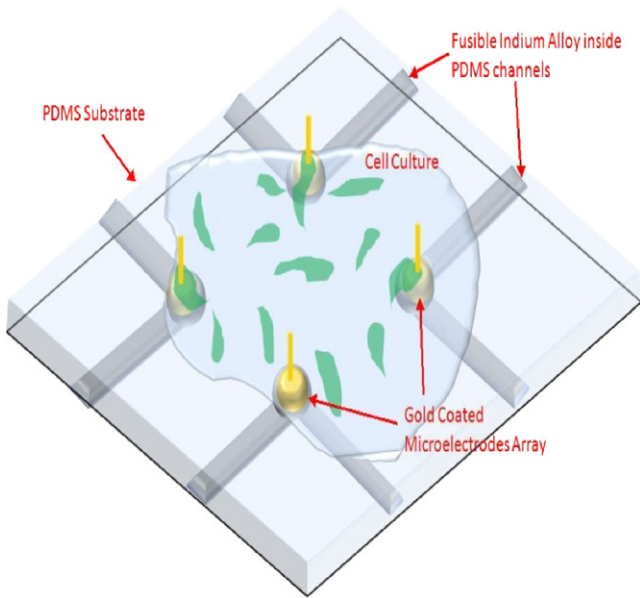


Figure 1. Schematic of the stretchable cell culture platform with embedded electrodes.

this platform we introduce significant improvements upon our previously reported stretchable microelectrode array [10]. In

section 2, we describe the platform structure and fabrication process followed by bench-top electrical characterizations in section 3. Section 4 discusses *in vitro* cell culture tests using smooth muscle cells and cardiomyocytes. Finally, in section 5, we conclude by summarizing important results.

2. Platform structure and fabrication process

Figure 1 shows a schematic of the cell culture platform, which consists of two PDMS layers. The top layer incorporates sub-surface liquid-alloy-filled microchannels and provides a biocompatible exterior surface for cell culture. The bottom layer is bonded to the top layer, sealing the microchannels. Gold-coated nail-head pins act as electrodes and are placed in the channels with their sharp heads protruding through the top PDMS layer. Their flange-shaped nail-head bottoms are flush against the underside of the top PDMS layer, sealing the junction against the leakage of alloy into the culture medium. Due to their larger size, gold pin electrodes are suitable for gross electrical recording and stimulation. Alternately, instead of gold pin electrodes, one can use smaller tungsten micro-wires, which are more suitable for single-cell field potential pick-ups and localized stimulation. Tungsten is exclusively used for single-cell recordings in the central nervous system,

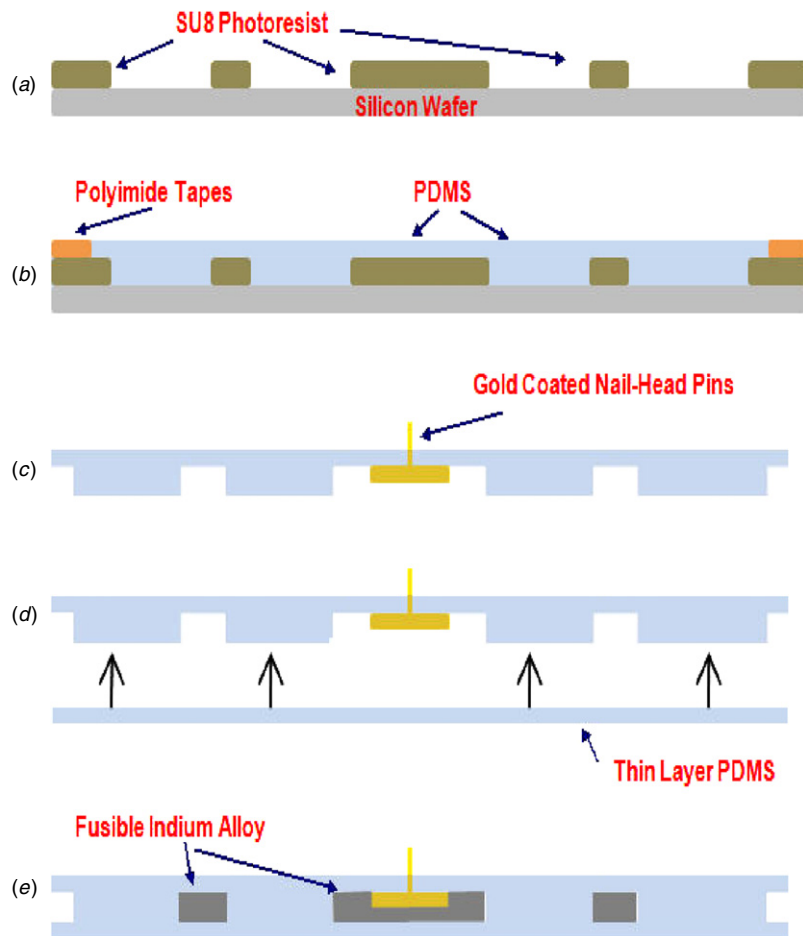


Figure 2. Fabrication process for the stretchable electrodes, (a) SU8 mold for the top layer incorporating the microchannels, (b) PDMA cast, (c) PDMS release and electrode insertion, (d) bond to the PDMS base layer, and (e) injection of indium alloy into the microchannels.

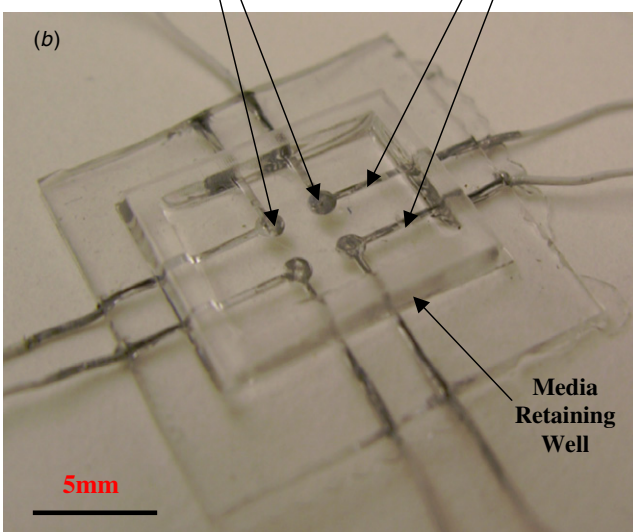
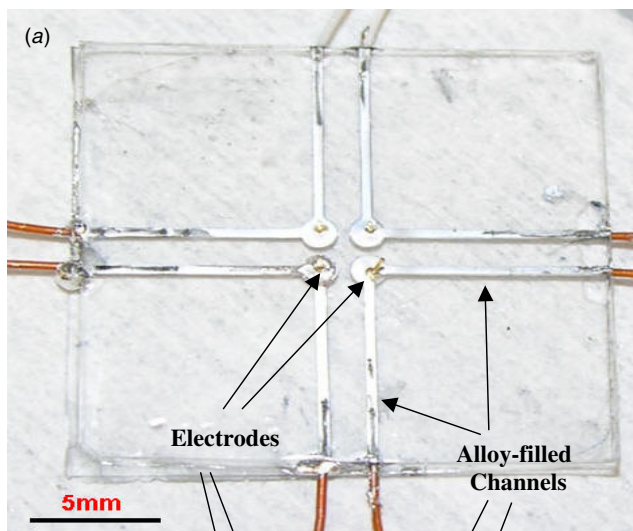


Figure 3. Photograph of a 4-channel stretchable platform with (a) gold pin electrodes and (b) tungsten micro-wire electrodes.

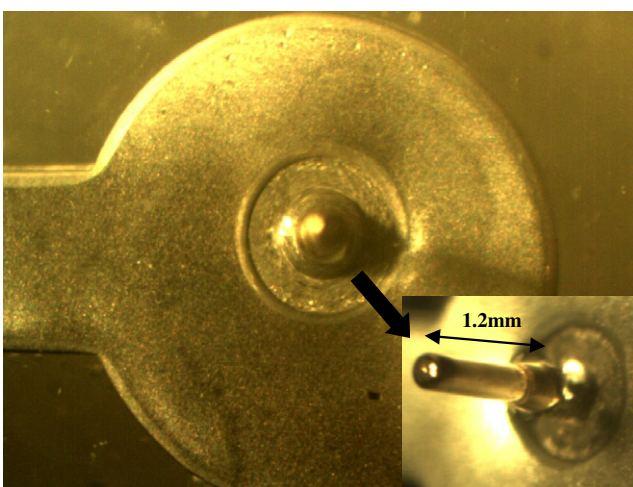


Figure 4. Gold nail-head pin electrode under a microscope under 30% strain; the inset clearly shows the PDMS neck around the pin, and its mechanical and chemical properties are well suited for integration into the stretchable platform.

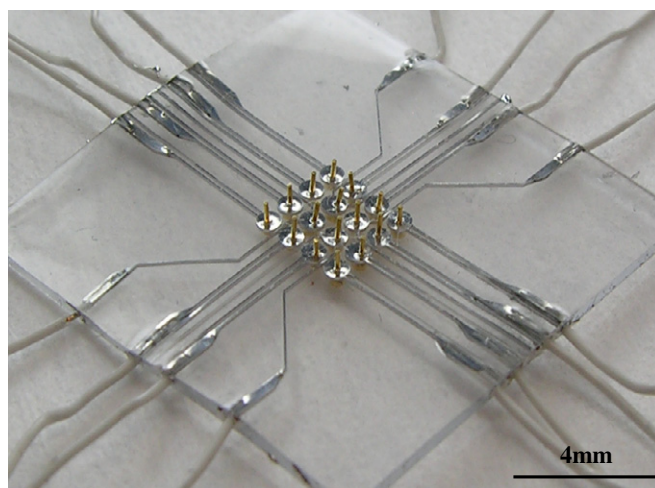


Figure 5. Photograph of a 16-channel gold-pin electrode array.

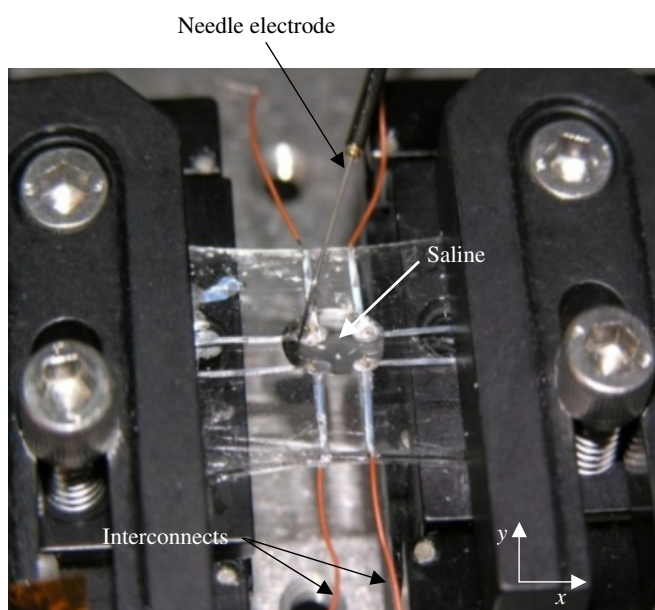


Figure 6. Stretch test setup using a micro-manipulator (stretched in the *x* direction while the impedance is measured between the needle electrode and gold pins).

Figure 2 shows the fabrication process for a platform with gold pin electrodes. It starts with an SU-8 mold (SU-8 2150, MicroChem Inc.) on a silicon wafer defining the microchannels (600 μm height, 500 μm width) and electrode placement areas, figure 2(a). Subsequently, uncured PDMS (800 μm thickness) is cast against the mold with polyimide tapes (200 μm) as spacers, figure 2(b). After release, the gold-coated nail-head pins (250 μm tip diameter and 750 μm head diameter, Mill-Max MFG Corporation) are inserted in electrode locations, figure 2(c). Another thin PDMS layer (300 μm in thickness) treated with a high-frequency charge generator (BD-10A, Electro-Technic Products, Inc.) is bonded to the top layer, figure 2(d). The bonded layers are kept at room temperature under atmospheric pressure for 24 h to ensure a strong interfacial bond. Finally,

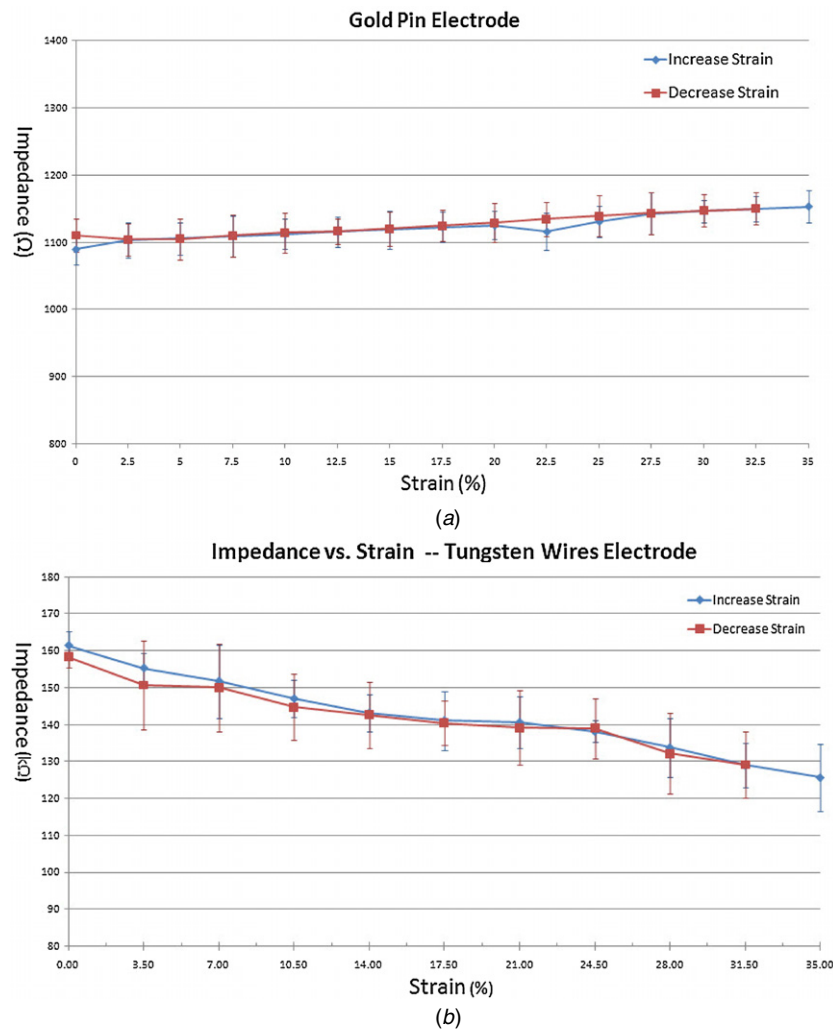


Figure 7. Strain versus impedance measurement results (a) for a gold pin electrode (constant versus strain), (b) for a tungsten electrode (impedance decrease is due to the exposure of more surface area at the junction between the tungsten and PDMS).

the room-temperature liquid indium alloy (gallium/indium = 75.5/24.5, liquidus temperature ≥ 15.7 °C, Indium Corporation, Utica, NY) is injected into the channels and thin connecting wires are inserted into the inlet and outlet ports for electrical connections, figure 2(e). Another room-temperature liquid alloy is the indium/mercury reported by Russell *et al* [11]. However, due to the environmental concerns over mercury, this alloy is not commercially available.

Figure 3(a) shows a photograph of the fabricated device with four electrodes. The device has total area of 25.4×25.4 mm² with an inter-electrode separation of 1.75 mm. The inlet and outlet ports are encapsulated with small PDMS droplets to prevent the leakage and oxidation of fusible indium alloy. As mentioned above, gold pins can be used for pacing applications (low impedance), while stiff tungsten micro-wires can be used for single-cell recording. Figure 3(b) shows a platform with four tungsten micro-wire electrodes ($25.4 \mu\text{m}$ in diameter). For the electrode shown in figure 3(b), the protruding tungsten micro-wires are cut flush to the PDMS surface. This is done to reduce the exposed surface area and hence increase the impedance to 100–200 k Ω for a more selective recording capability.

Insertion of the gold pin electrode through PDMS provides a self-sealed junction through the creation of an elastomeric collar around the shaft of the electrode. Figure 4 shows an optical micrograph of a gold pin inserted into the PDMS top cover. As can be seen, a PDMS ring is formed around the base with extensions (300–400 μm in height) covering the neck of the pin (figure 4, inset). This PDMS ring/collar adhesive provides an excellent barrier against any leakage of indium alloy under the electrode area during mechanical deformation. Since additional sealing steps are unnecessary, the device assembly requires a minimum of manual manipulation.

The fabrication technique discussed above is scalable to higher density electrode arrays. The factors limiting the scaling are the smallest channel dimensions that can be easily filled with indium alloy and the diameter of the electrodes. We successfully injected the room-temperature liquid alloy into PDMS microchannels with 50 μm width. We did not attempt to fill channels below 50 μm (although we think it is possible to fill smaller channels) since below that limit the size of the electrodes prohibits denser packing. Figure 5 shows 16-channel gold pin electrodes with an inter-electrode separation of 150 μm . As can be seen, in this case the limiting factor is

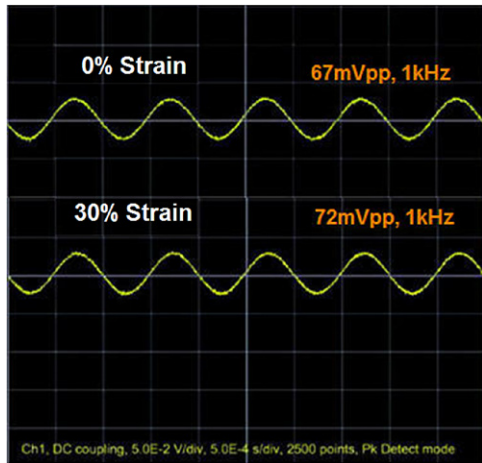


Figure 8. Recorded signals through agarose gel (top: signal recorded at 0% strain; bottom: signal recorded at 30% strain).

mainly the size of the electrodes. In our experiments, we used the smallest commercially available pins; a higher density electrode array is obtainable by using tungsten micro-wires or through a more complicated fabrication process such as through-PDMS electroplated gold electrodes.

3. Bench-top electrical characterizations

The stretchable electrode array, without cells, was attached to a micro-manipulator in order to evaluate its electrical properties, i.e. interconnect resistance as a function of applied strain. Figure 6 illustrates the stretch test experimental setup. The device was clamped to a pair of micromanipulators with a droplet of phosphate buffer saline ($\text{pH} = 7.4$) placed on the device covering the electrodes. The impedance was measured between electrodes and the needle (four electrodes were measured individually and the impedance value's mean and standard deviations were calculated) at 1 kHz with the platform stretched by 2.5% strain increments and decrements. Figure 7(a) shows strain versus impedance measurement results for gold pin electrodes showing a constant impedance of $\sim 1.1 \text{ k}\Omega$ with applied strains of up to 35%. Figure 7(b) shows strain versus impedance measurements for the tungsten electrodes showing a drop from 160 $\text{k}\Omega$ for the unstrained platform to 125 $\text{k}\Omega$ at 35% strain. This is due to exposure of a larger tungsten area around the neck of the electrode (as mentioned above, for these electrodes, the protruding tungsten microwires were cut flush to the PDMS surface, hence the reason for extra area exposure with increased strain). We performed reliability tests by subjecting the platform to 100 cycles of stretch–release (0–40%), after which, the electrical tests were performed again; we did not observe any alloy leakage or electrode breakage.

In addition to saline tests, we also performed measurements using agarose gel (0.2% w/v) to mimic a brain tissue slice [12]. The agarose gel was placed on the stretchable electrode array platform within a PDMS ring container. The entire platform was clamped to a pair of micro-manipulators with a probe inserted into the agarose gel. A sinusoidal

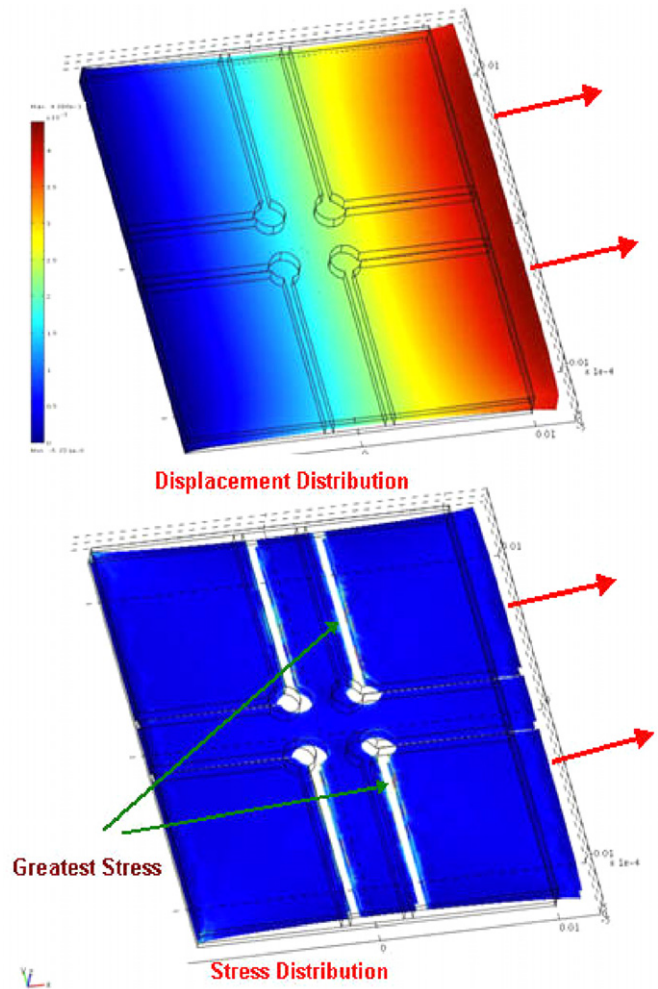


Figure 9. Simulation results for displacement and stress distribution of the stretchable electrode array. Stress concentration is along the channels in the direction perpendicular to the applied force.

signal (100 mVpp, 1 kHz) was applied to the probe and transmitted voltages were recorded through gold-coated nail-head electrodes. Figure 8 shows the recorded waveforms at 0% and 30% strain. The slight difference in signal amplitude between 0% and 30% (67–72 mVpp) could be due to the deformation of agarose gel. The results clearly demonstrate the recording capability of the stretchable electrode array platform through tissue phantoms.

Mechanical strain beyond 40% resulted in the breakage of the PDMS platform along the microchannels in the direction perpendicular to the applied force. COMSOL® finite element simulations verified this phenomenon. Figure 9 shows displacement and stress simulations assuming a Young's modulus and tensile strength of 750 kPa and 2.24 MPa for PDMS (1:10 mixing ratio), respectively [13, 14]. The device was fixed at the left end and the red arrows indicate the direction of applied displacement (4.4 mm, 22% strain) in the x -direction. As expected, the displacement increases linearly in the x -direction resulting in a uniform stress distribution across most of the platform except the channel boundary regions which are subjected to an increased stress (30 times increase as compared to other areas). In this case

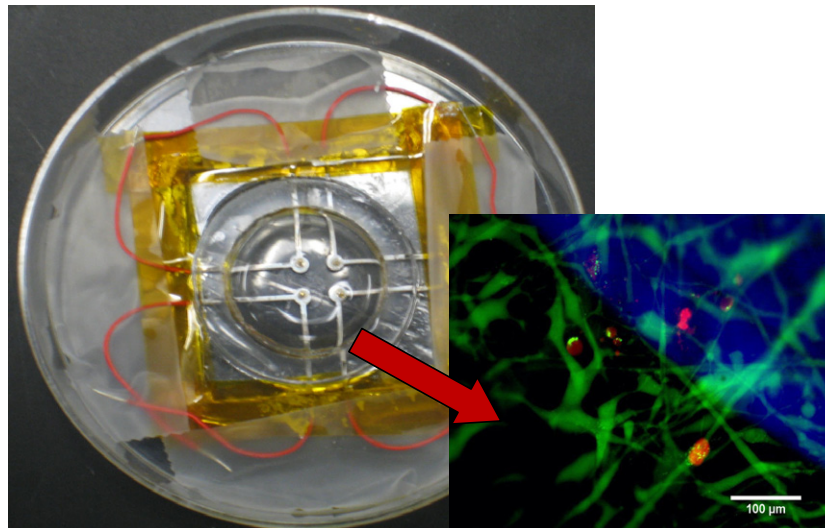


Figure 10. Stretchable cell culture platform populated with human aortic smooth muscle cells enclosed by PDMS retaining ring after 2 days of incubation. Live/dead staining (shown in the inset) indicated that the device was biocompatible as the vast majority of cells survived (green) while relatively few died (red).

(22% strain), the maximum strain at the channel boundary exceeds the tensile strength indicating a breakage point. We should mention that the discrepancy between the simulated and measured results (22% versus 40%) is due to the wide variability in the mechanical properties of PDMS. The values we chose for the simulation can be different from the values of the actual device depending on the amount of cross-linker and curing conditions. Young's modulus of PDMS decreases as the amount of curing (i.e. cross linker) agent is reduced (860 kPa for 1:5 mixing ratio and 360 kPa for 1:15 mixing ratio) [15]. In addition to the variations of Young's modulus with cross-linker density, it has recently been reported that the PDMS mechanical strength Young's modulus is also thickness dependent, i.e. they both decrease with increasing thickness [16].

4. *In vitro* cell culture experiments

Cell culture experiments with live/dead assay (Invitrogen L3224) were performed to confirm hermeticity of indium alloy inside the PDMS channels. PDMS retaining rings on the devices created a sealed region for cell culture media, figure 10. Devices were prepared by coating the top surface with 2% gelatin after O₂ plasma surface activation. Human aortic smooth muscle cells were then plated on the devices. The inset in figure 10 shows the fluorescent microscopic image of the aortic smooth muscle cells after 2 days of culture. Since the majority of cells survived (green) and relatively few died (red), short-term biocompatibility was demonstrated. Figure 11 shows that these cells stretched to 10% strain. As can be seen, cells remained viable and attached to the PDMS surface even during stretch.

In order to demonstrate the functionality of the gold pin platform with cultured cells, we performed electrical pacing of isolated adult murine cardiomyocytes. The cell population was prepared and deposited on the device allowing

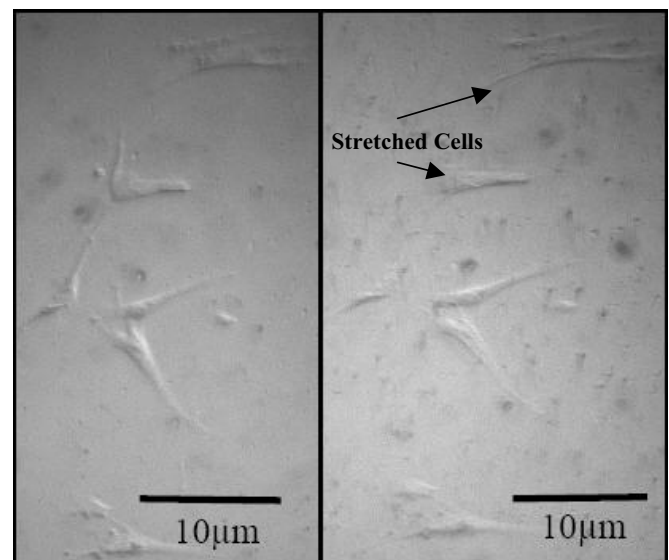


Figure 11. Smooth muscle cells remain attached to the platform and stretch with it upon the application of 10% strain.

30–90 min for cell attachment. Then the buffer medium containing non-attached cells was aspirated and Tyrode's salt solution was added to the PDMS ring wells shown in figure 10. Following the preparation of cardiomyocytes, device wires were connected to a commercial electrical pacer (MyoPacer, IonOptix LLC). A biphasic signal (± 15 V, 10 ms, 1 Hz) was then applied resulting in contraction of cardiomyocytes on the surface, demonstrating that the device could be utilized for *in vivo* stimulation.

To demonstrate the functionality of the tungsten wire platform, we stimulated murine embryonic stem cell-derived cardiomyocytes with the tungsten microelectrodes. The tungsten micro-wire platform was adapted for use with a commercial microelectrode array system (Multi Channel Systems, Reutlingen, Germany). To enable electrical

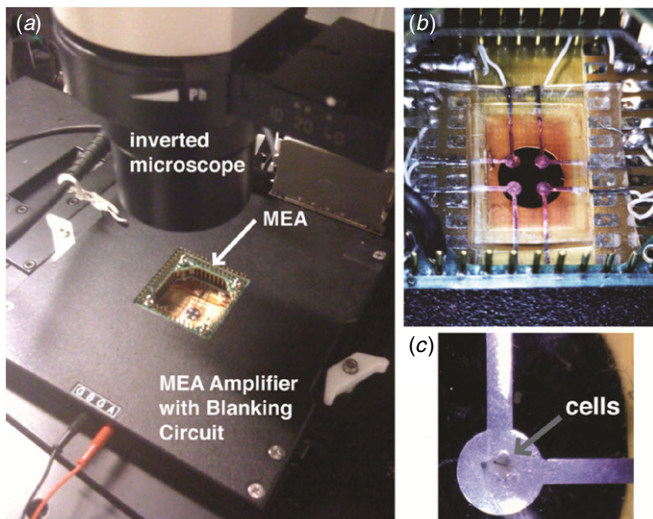


Figure 12. Electrical sensing measurements were made by adapting the stretchable MEA for use with a commercial microelectrode array system. (a) The stretchable MEA is connected to the commercial MEA amplifier system and viewed with an inverted microscope. (b) Details of the stretchable MEA. (c) Beating cell clusters were manually positioned directly on top of tungsten microwires to enable a cell-micro-wire contact.

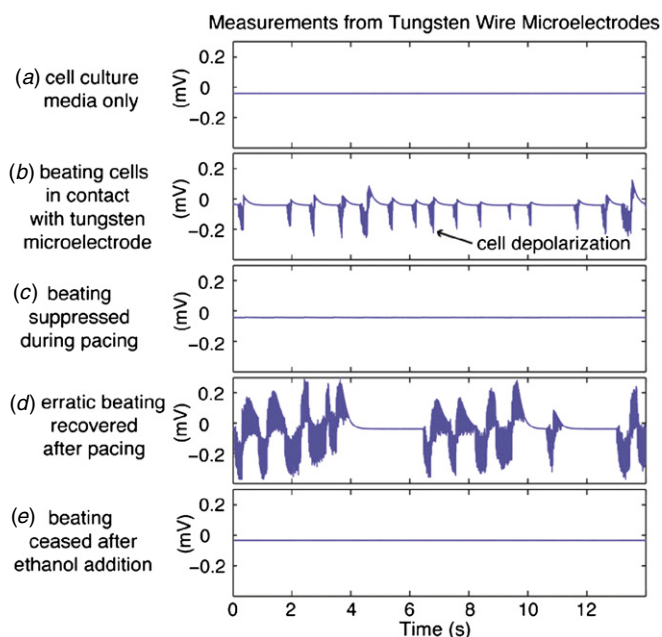


Figure 13. (a) No signal was observed with cell culture media only, but when spontaneously contracting cardiomyocytes were brought into contact with the tungsten microelectrodes, (b) single depolarization of around -0.2 mV was observed. Pacing suppressed contractions (c) and recovery of beating was observed once pacing was stopped (d). After the addition of ethanol to kill the cells, beating ceased (e).

contact between the stretchable microelectrode array and the commercial amplifier system, an acrylic adapter plate with copper contacts was fabricated (see figure 12). Custom LabView software was used to stimulate and record from the microelectrode array. For cell experiments, embryoid body clusters of differentiated murine embryonic stem cells were

monitored for the presence of beating cells. Beating colonies were harvested and seeded onto a gelatin-coated device in cell culture media (15% fetal bovine serum). Cells were allowed to attach for 1 h before pacing experiments.

In order to measure single-cell depolarizations, the cardiomyocytes had to be directly in contact with the tungsten microelectrode. This required careful cell placement, but then a strong signal was observed (see figure 13). The noise floor of the device with media only was less than $2 \mu\text{V}$, while signals around 0.2 mV were observed when beating cells were in contact with the electrodes. External platinum pacing electrodes were used to apply electric field stimulation, but pacing actually suppressed cell beating. Future work will focus on successfully pacing these cells and recording the resulting depolarizations. After stimulation was stopped the beating recovered but was somewhat erratic. As a final demonstration that the cell depolarizations were responsible for the observed signal, we added ethanol to the cell media, killing the cells, and we observed immediate cessation of the depolarization signal and a return to the ‘media only’ flat trace.

5. Conclusions

We designed a simple and cost-effective process for fabricating a stretchable microelectrode array using PDMS, room-temperature liquid alloy, and gold-coated nail-head pins or tungsten micro-wires. The stretchability exceeds what has been reported in the literature for gold-PDMS combination electrodes. We demonstrated device biocompatibility and functionality by culturing human aortic smooth muscle cells and pacing of adult murine cardiomyocytes. The cells adhered well to the substrate during mechanical strain and survived near and on the electrodes after 2 days of incubation. The platform also maintained its electrical capabilities after being subjected to repeated cycles of mechanical deformation. Finally, we demonstrated the electrical functionality of the gold pin system by pacing primary adult murine cardiomyocytes, and we used the tungsten wire platform in conjunction with a commercial amplifier system to record single-cell depolarization from murine embryonic stem cell-derived cardiomyocytes. This platform holds potential for use in both dynamic *in vivo* and *in vitro* applications.

Acknowledgments

The authors would like to thank the staff at the Purdue University Birck Nanotechnology Center for their assistance in fabrication. The authors would also like to thank Ali Rastegar for his generous help solving electrical problems involved in the integration of the stretchable MEA with the commercial amplifier system. The authors would like to acknowledge support from the National Institutes of Health (R21-EB005351 and R21-HL089027), the National Science Foundation (EFRI 0735551 and CAREER ECS-0449400), the California Institute of Regenerative Medicine (RC1-00151), and Stanford University (Bio-X Graduate Fellowship and DARE Doctoral Fellowship).

References

- [1] Lacour S P, Benmerah S, Tarte E, FitzGerald J, Serra J, McMahon S, Fawcett J, Graudejus O, Yu Z and Morrison B 2010 Flexible and stretchable micro-electrodes for *in vitro* and *in vivo* neural interfaces *Med. Biol. Eng. Comput.* **48** 945–54
- [2] Lacour S P, Tsay C, Wagne S, Zhe Y and Morrison B 2005 Stretchable micro-electrode arrays for dynamic neuronal recording of *in vitro* mechanically injured brain *Proc. IEEE Sensors Conf. (Irvine, CA)* pp 617–20
- [3] Saha S, Ji L, de Pablo J J and Palecek S P 2006 Inhibition of human embryonic stem cell differentiation by mechanical strain *J. Cell. Physiol.* **206** 126–37
- [4] Lee I C, Wang J H, Lee Y T and Young T H 2007 The differentiation of mesenchymal stem cells by mechanical stress or/and co-culture system *Biochem. Biophys. Res. Commun.* **352** 147–52
- [5] Maghribi M, Hamilton J, Polla D, Rose K, Wilson T and Krulevitch P 2002 Stretchable micro-electrode array (for retinal prosthesis) *Proc. 2nd Annu. Int. IEEE-EMB Special Topic Conf. on Microtechnologies in Medicine & Biology (Madison, WI)* pp 80–3
- [6] Tsay C, Lacour S P, Wagner S and Morrison B 2005 Architecture, fabrication, and properties of stretchable micro-electrode arrays *Proc. IEEE Sensors Conf. (Irvine, CA)* pp 1169–72
- [7] Schuettler M, Pfau D, Ordonez J S, Henle C, Wois P and Steiglitz T 2009 Stretchable tracks for laser-machined neural electrode arrays *Proc. 31st Int. Conf. of the IEEE EMBS (Minneapolis, MN)* pp 1612–5
- [8] Jones J, Lacour S P, Wagner S and Suo Z 2004 Stretchable wavy metal interconnects *J. Vac. Sci. Technol. A* **22** 1723–5
- [9] Lacour S P, Jones J, Suo Z and Wagner S 2004 Design and performance of thin metal film interconnects for skin-like electronic circuits *IEEE Electron Device Lett.* **25** 179–81
- [10] Wei P, Taylor R E, Ding Z, Higgs G, Norman J J, Pruitt B L and Ziaie B 2009 A stretchable cell culture platform with embedded electrode array *Proc. IEEE MEMS Conf. (Sorrento, Italy)* pp 407–10
- [11] Russell S S and Levine S L 1970 Indium-mercury alloy as a low-toxicity liquid electrode *IBM J. Res. Dev.* **14** 70–1
- [12] Chen Z J, Gillies G T, Broaddus W C, Prabhu S S, Fillmore H, Mitchell R M, Corwin F D and Fatouros P P 2004 A realistic brain tissue phantom for intraparenchymal infusion studies *J. Neurosurg.* **101** 312–22
- [13] <http://www.mit.edu/~6.777/matprops/pdms.htm> (accessed October 2010)
- [14] Furad D, Tzvetkova-Cheolleau T, Decossas S, Tracqui P and Schiavone P 2008 Optimization of poly-di-methyl-siloxane (PDMS) substrates for studying cellular adhesion and motility *Microelectron. Eng.* **85** 1289–93
- [15] Armani D, Liu C and Aluru N 1999 Re-configurable fluid circuits by PDMS elastomer micromachining *Proc. IEEE MEMS Conf. (Orlando, FL)* pp 222–7
- [16] Liu M, Sun J, Sun Y, Block C and Chen Q 2009 Thickness-dependent mechanical properties of polydimethylsiloxane membranes *J. Micromech. Microeng.* **19** 035028